

# IUCrJ

**Volume 5 (2018)**

**Supporting information for article:**

**Structures of collagen IV globular domains: insight into associated pathologies, folding and network assembly**

**Patricia Casino, Roberto Gozalbo-Rovira, Jesús Rodríguez-Díaz, Sreedatta Banerjee, Ariel Boutaud, Vicente Rubio, Billy G. Hudson, Juan Saus, Javier Cervera and Alberto Marina**

**Table S1** Primers used for  $\alpha$ NC1 amplification.

Product	Primer name	Primer sequences
$\alpha$ 1(IV)NC1	NCI1_Flag1/2_FWD	GACAAGGGCCCCGATGGGTTGCCAGGATCCATGGGGCCC
	NCI1_Flag_FWD	GACTACAAGGACGACGATGACAAGGGCCCCGATGGGTTGCCAGGATCC
	NCI1_REV	TAGCTGAGTCAGGCTTCATTATGTTCT
	NCI1_KpnI_REV	CCATGTTGGTACCTTAGCTGAGTCAGGCTTCATTATGTTCT
$\alpha$ 2(IV)NC1	NCI2_Flag1/2_FWD	GACAAGGGCCGTCCAGGGAGCCCCGGCCTGCCGGGTATG
	NCI2_Flag_FWD	GACTACAAGGACGACGATGACAAGGGCCGTCCAGGGAGC
	NCI2_REV	TTCCTGGCACGCGCCGGCTCACAGTT
	NCI2_SacI_REV	TTCCTGGCAGAGCTCGGCTCACAGTT
$\alpha$ 4(IV)NC1	NCI4_Flag1/2_FWD	GACAAGCTAGCTGGTCCCATTGGGGATCCTGGGCCAAA
	NCI4_Flag_FWD	GACTACAAGGACGACGATGACAAGCTAGCTGGTCCCATTGGGGATCCTGGGCC
	NCI4_REV	GCCGAGGGCCCCTAGCTATACTTCACGCAG
	NCI4_KpnI_REV	ATTGGTACCGCCGAGGGCCCCTAGCTA
$\alpha$ 5(IV)NC1	NCI5_Flag1/2_FWD	GACAAGGGTCCAGATGGATTGCAAGGTCCCCAGGTCCC
	NCI5_Flag_FWD	GACTACAAGGACGACGATGACAAGGGTCCAGATGGATTGCAAGGTCCC
	NCI5_Flag_REV	AAGGAATTCTTCAAATGTTATGTCCT
	NCI5_SacI_REV	GGTGAGCTCAAGGAATTCTTCAAAAATG
Cloning Bm40 and Flag	Flag_SignalP1_FWD	AGGGCTCTGGCAGCCCCACTAGCCGACTACAAGGACGACGATGACAAG
	SignalP1_SignalP2_FWD	TTCTTTCTCCTTTGCCTGGCCGGGAGGGCTCTGGCAGCCCCACTAGCC
	SignalP2_BamHI_FWD	AGGGGGATCCATGAGGGCCTGGATCTTCTTCTCCTTTGCCTG
	SignalP2_XhoI_FWD	AGGGCTCGAGATGAGGGCCTGGATCTTCTTCTCCTTTGCCTG

**Table S2** Residue numbers for the structures of  $\alpha$ 1,  $\alpha$ 2,  $\alpha$ 3,  $\alpha$ 4 and  $\alpha$ 5 NC1 domains and their corresponding residue numbers according to the UniprotKB accession number.

Collagen $\alpha$ (IV) NC1 domain	Residue numbers in each chain	Corresponding residue numbers in the complete $\alpha$ (IV) chain	
		UniprotKB accession number	Residue number
$\alpha$ 1NC1	1-229	P02462	1441-1669
$\alpha$ 2NC1	1-228	P08572	1485-1712
$\alpha$ 3NC1	1-230	Q01955	1441-1671
$\alpha$ 4NC1	1-230	P53420	1461-1690
$\alpha$ 5NC1	1-229	P29400	1461-1685

**Table S3** Root mean square deviations (r.m.s.d.), in Å, for the superposition of the structures of NC1 hexamers.

The number of Ca atoms superimposed is indicated between parentheses.

Rmsd (Å)	$\alpha 1\text{NC1}_{\text{homo}}$	$\alpha 3\text{NC1}_{\text{homo}}$	$\alpha 5\text{NC1}_{\text{homo}}$	$\alpha 121\text{NC1}$	$\alpha 121\text{NC1}(\text{PDB:1LI1})^*$
$\alpha 1\text{NC1}_{\text{homo}}$	-	0.62 (1342)	0.55 (1356)	0.59 (1335)	0.73 (1346)
$\alpha 3\text{NC1}_{\text{homo}}$		-	0.67 (1344)	0.72 (1327)	0.84 (1329)
$\alpha 5\text{NC1}_{\text{homo}}$			-	0.67 (1338)	0.70 (1338)
$\alpha 121\text{NC1}$				-	0.48 (1348)

\*Human  $\alpha 121\text{NC1}$  obtained from placenta, PDB file 1LI1.

**Table S4** Root mean square deviations (r.m.s.d.), in Å, for the superposition of the structures of the various recombinant NC1 chains crystallized here and the  $\alpha 1$ -2NC1 chains of human placenta.

The number of Ca atoms superimposed is indicated between parentheses.

Rmsd (Å)	$\alpha 1\text{NC1}_{\alpha 121}$	$\alpha 2\text{NC1}^*$	$\alpha 2\text{NC1}_{\alpha 121}$	$\alpha 2\text{NC1}_{\text{homo}}$	$\alpha 3\text{NC1}_{\text{homo}}$	$\alpha 4\text{NC1}_{\text{homo}}$	$\alpha 5\text{NC1}_{\text{homo}}$
$\alpha 1\text{NC1}^*$	0.35 (226)				0.65 (224)		0.47 (226)
$\alpha 1\text{NC1}_{\alpha 121}$	-		0.75 (218)	1.44 (166)	0.53 (225)	1.27 (178)	0.41 (226)
$\alpha 2\text{NC1}^*$		-	0.45 (224)	1.20 (169)		1.27 (174)	
$\alpha 2\text{NC1}_{\alpha 121}$	0.84 (219)	0.45(224)		1.22 (168)	0.88 (219)	1.25 (175)	0.79 (219)
$\alpha 1\text{NC1}_{\text{homo}}$	0.36 (226)				0.53(225)		0.41 (226)
$\alpha 2\text{NC1}_{\text{homo}}$		-	-	-	1.45 (167)	1.40 (164)	1.46 (167)
$\alpha 3\text{NC1}_{\text{homo}}$					-	1.26 (179)	0.58 (225)
$\alpha 4\text{NC1}_{\text{homo}}$						-	1.23 (178)
$\alpha 5\text{NC1}_{\text{homo}}$							-

\*From human placenta, PDB file 1LI1.

**Table S5** Missense mutations found in Alport's syndrome patients in  $\alpha$ 5NC1,  $\alpha$ 3NC1 and  $\alpha$ 4NC1.  $\alpha$ 5NC1 mutations have been extracted from The Alport syndrome COL4A5 variant database ([www.arup.utah.edu/database/ALPORT/ALPORT\\_welcome.php](http://www.arup.utah.edu/database/ALPORT/ALPORT_welcome.php)).

The mutations in chains  $\alpha$ 3NC1 and  $\alpha$ 4NC1 were reported in the publications given as footnotes to the Table.

Protein Change	Protein residue	$\alpha$ NC1
p.Cys1476Phe	C20F	$\alpha$ 5NC1
p.Thr1480Arg	T24R	$\alpha$ 5NC1
p.Gly1486Ala	G30A	$\alpha$ 5NC1
p.Ser1488Phe	S32F	$\alpha$ 5NC1
p.Ala1498Asp	A42D	$\alpha$ 5NC1
p.Arg1511His	R55H	$\alpha$ 5NC1
p.Pro1517Thr	P61T	$\alpha$ 5NC1
p.Trp1538Ser	W82S	$\alpha$ 5NC1
p.Pro1559Ala	P103A	$\alpha$ 5NC1
p.Arg1563Gln	R107Q	$\alpha$ 5NC1
p.Cys1564Arg	C108R	$\alpha$ 5NC1
p.Cys1564Ser	C108S	$\alpha$ 5NC1
p.Cys1567Arg	C111R	$\alpha$ 5NC1
p.Cys1567Ser	C111R	$\alpha$ 5NC1
p.Glu1568Gln	E112Q	$\alpha$ 5NC1
p.Pro1584Leu	P128L	$\alpha$ 5NC1
p.Cys1586Arg	C130R	$\alpha$ 5NC1
p.Cys1586Phe	C130F	$\alpha$ 5NC1
p.Gly1589Val	G133V	$\alpha$ 5NC1
p.Trp1590Gly	W134G	$\alpha$ 5NC1
p.Gly1596Asp	G140D	$\alpha$ 5NC1
p.Tyr1597Cys	Y141C	$\alpha$ 5NC1
p.Met1601Ile	M145I	$\alpha$ 5NC1
p.Leu1621Ser	L165S	$\alpha$ 5NC1
p.Cys1632Gly	C176G	$\alpha$ 5NC1
p.Cys1632Trp	C176W	$\alpha$ 5NC1
p.Cys1638Tyr	C182Y	$\alpha$ 5NC1
p.Leu1649Arg	L193R	$\alpha$ 5NC1
p.Ser1659Asn	S203N	$\alpha$ 5NC1
p.Arg1677Gln	R221Q	$\alpha$ 5NC1
p.Arg1677Pro	R221P	$\alpha$ 5NC1
p.Arg1677Leu	R221L	$\alpha$ 5NC1
p.Cys1678Arg	C222R	$\alpha$ 5NC1
p.Cys1678Trp	C222W	$\alpha$ 5NC1
p.Gln1679Pro	Q223P	$\alpha$ 5NC1
p.Cys1681Phe	C225F	$\alpha$ 5NC1
p.Gly1508Ser <sup>1</sup>	G48S	$\alpha$ 4NC1
p.Cys1513Thr <sup>1</sup>	C53T	$\alpha$ 4NC1
p.Cys1588Thr <sup>1</sup>	C128T	$\alpha$ 4NC1
p.Leu1474Pro <sup>2</sup>	L34P	$\alpha$ 3NC1
p.Leu1474Cys <sup>3</sup>	L34C	$\alpha$ 3NC1

p.Phe1475Ser <sup>4</sup>	F35S	$\alpha$ 3NC1
p.Cys1511Ile <sup>5</sup>	C71I	$\alpha$ 3NC1
p.Cys1548Tyr <sup>4</sup>	C108Y	$\alpha$ 3NC1
p.Val1550Gly <sup>4</sup>	V110G	$\alpha$ 3NC1
p.Trp1578Ser <sup>6</sup>	W138S	$\alpha$ 3NC1
p.Qln1495Arg <sup>6</sup>	Q156R	$\alpha$ 3NC1

<sup>1</sup> Storey, H., Savige, J., Sivakumar, V., Abbs, S., Flinter, F. A. (2013). *J Am Soc Nephrol* 24,1945-1954

<sup>2</sup> Lemmink, H. H., Mochizuki, T., van den Heuvel, L. P., Schröder, C. H., Barrientos, A., Monnens, L. A., van Oost, B. A., Brunner, H. G., Reeders, S. T., Smeets, H. J. (1994). *Hum Mol Genet* 3,1269-1273.

<sup>3</sup> Mochizuki, T., Lemmink, H. H., Mariyama, M., Antignac, C., Gubler, M. C., Pirson, Y., Verellen-Dumoulin, C., Chan, B., Schröder, C. H., Smeets, H. J., Reeders, S. T. (1994). *Nat Genet* 8,77-81.

<sup>4</sup> Tazón Vega, B., Badenas, C., Ars, E., Lens, X., Milà, M., Darnell, A., Torra, R. (2003). *Am J Kidney Dis* 42, 952-959.

<sup>5</sup> Heidet, L., Arrondel, C., Forestier, L., Cohen-Solal, L., Mollet, G., Gutierrez, B., Stavrou, C., Gubler, M. C., Antignac, C. (2001). *J Am Soc Nephrol* 12, 97-106.

<sup>6</sup> Voskarides, K., Damianou, L., Neocleous, V., Zouvani, I., Christodoulidou, S., Hadjiconstantinou, V., Ioannou, K., Athanasiou, Y., Patsias, C., Alexopoulos, E., Pierides, A., Kyriacou, K., Deltas, C. (2007). *J Am Soc Nephrol* 18, 3004-3016

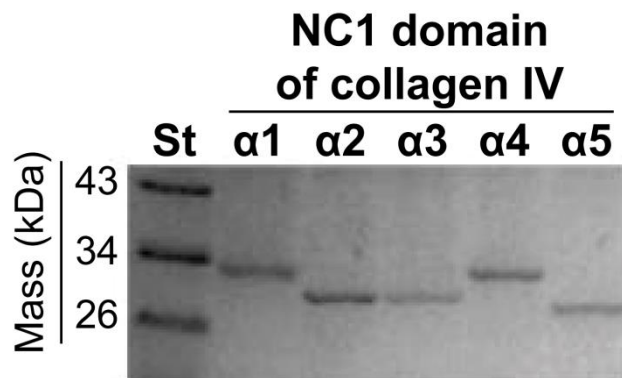


**Figure S1** Purified human  $\alpha$ 1-5NC1 domains produced by recombinant techniques. Coomassie-stained SDS-PAGE (12% polyacrylamide gel). St, protein standards

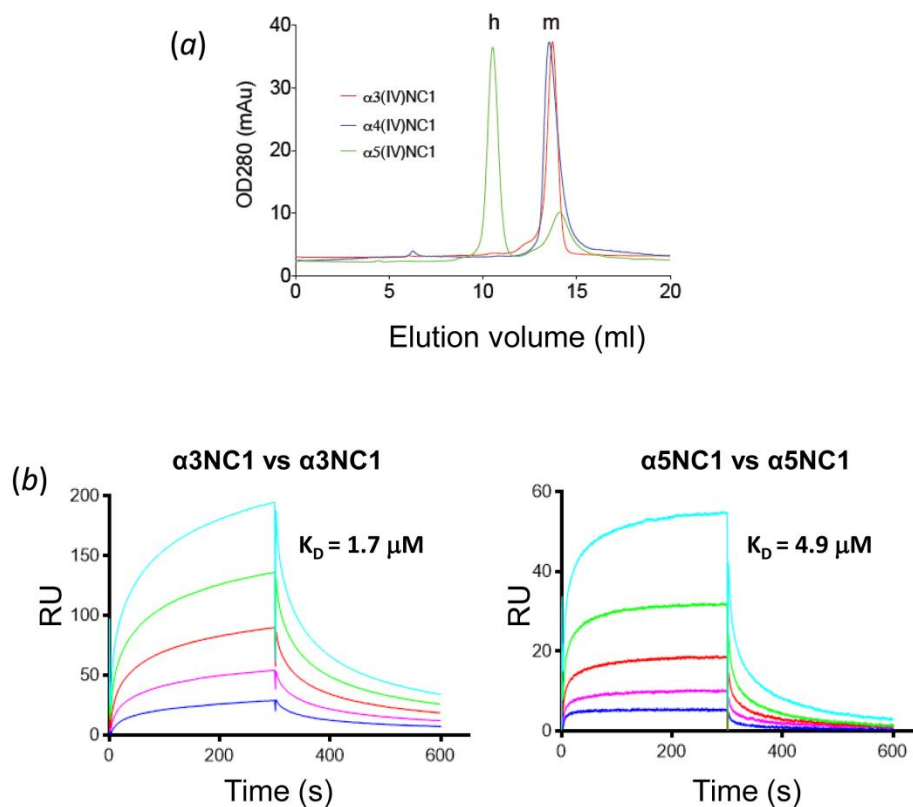


**Figure S2** *In vitro* evidence of self-association capacity of  $\alpha 3NC1$  and  $\alpha 5NC1$ . (a) Gel filtration chromatography of  $\alpha 3NC1$ ,  $\alpha 4NC1$  and  $\alpha 5NC1$ . "h" and "m" stand for hexamer and monomer, respectively. (b) Surface Plasmon Resonance assays.  $\alpha 3NC1$  (left) or  $\alpha 5NC1$  (right) covalently bound to the sensorchip were used in these assays; the ligands were the  $\alpha 3NC1$  (left) or  $\alpha 5NC1$  (right) chains in solution at concentrations (profiles from bottom to top) of 0.25, 0.5, 1, 2 and 4  $\mu M$ . The figure depicts examples of sensorchip traces after subtraction of blanks obtained simultaneously with protein-free solutions.  $K_D$  values were estimated from the obtained signal level, (average of two assays at least). For further details, see Materials and Methods.

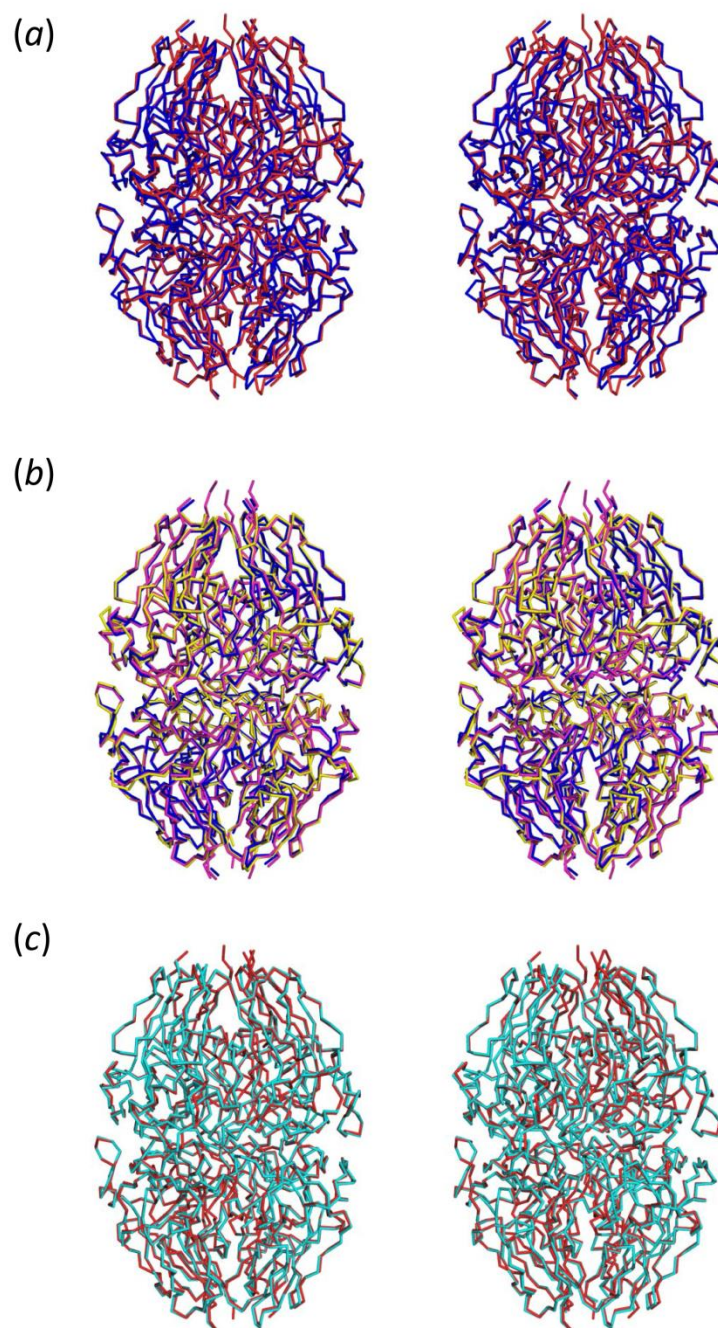


**Figure S3** Stereo views of the superimpositions of the backbone of NC1 structures. (a)  $\alpha 121\text{NC1}$  hexamer obtained from human placenta (PDB file 1LI1) (red) superimposed over  $\alpha 5\text{NC1}_{\text{homo}}$ . (b)  $\alpha 1\text{NC1}_{\text{homo}}$  (magenta),  $\alpha 3\text{NC1}_{\text{homo}}$  (yellow) and  $\alpha 5\text{NC1}_{\text{homo}}$  (blue) hexamers. (c)  $\alpha 121\text{NC1}$  hexamers obtained from placenta (red) or produced by recombinant techniques in this study (cyan).



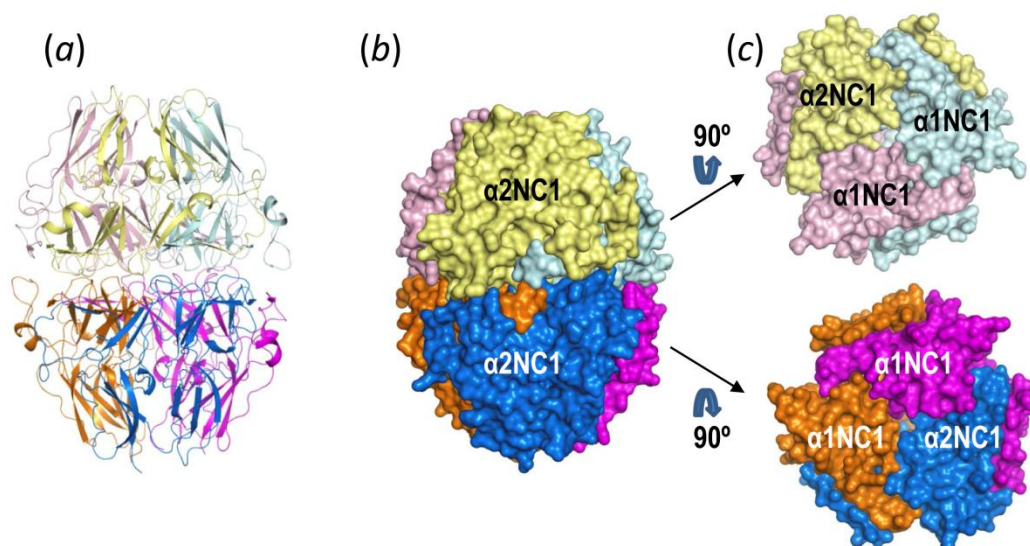


**Figure S4** Structure of recombinant  $\alpha 121\text{NC1}$  found in the asymmetric unit of its crystal: (a) cartoon representation or (b) surface representation, with each subunit showed with a different colour. In (c) the hexamer is deconstructed in its two protomers, viewed from their equatorial surfaces through which both trimers interact.

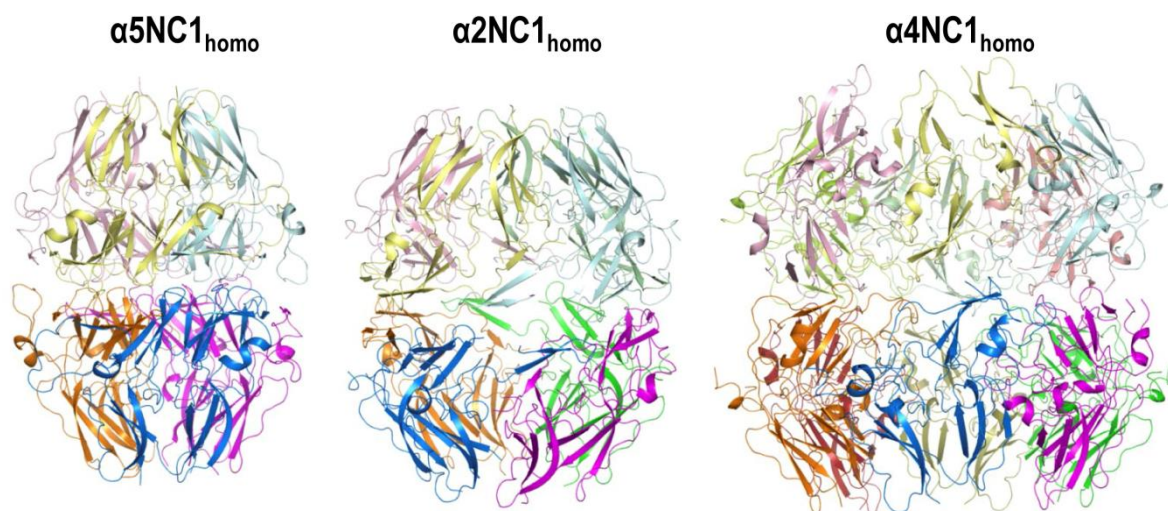


**Figure S5**

Cartoon representation of the oligomer quaternary structures for the indicated NC1 domains.



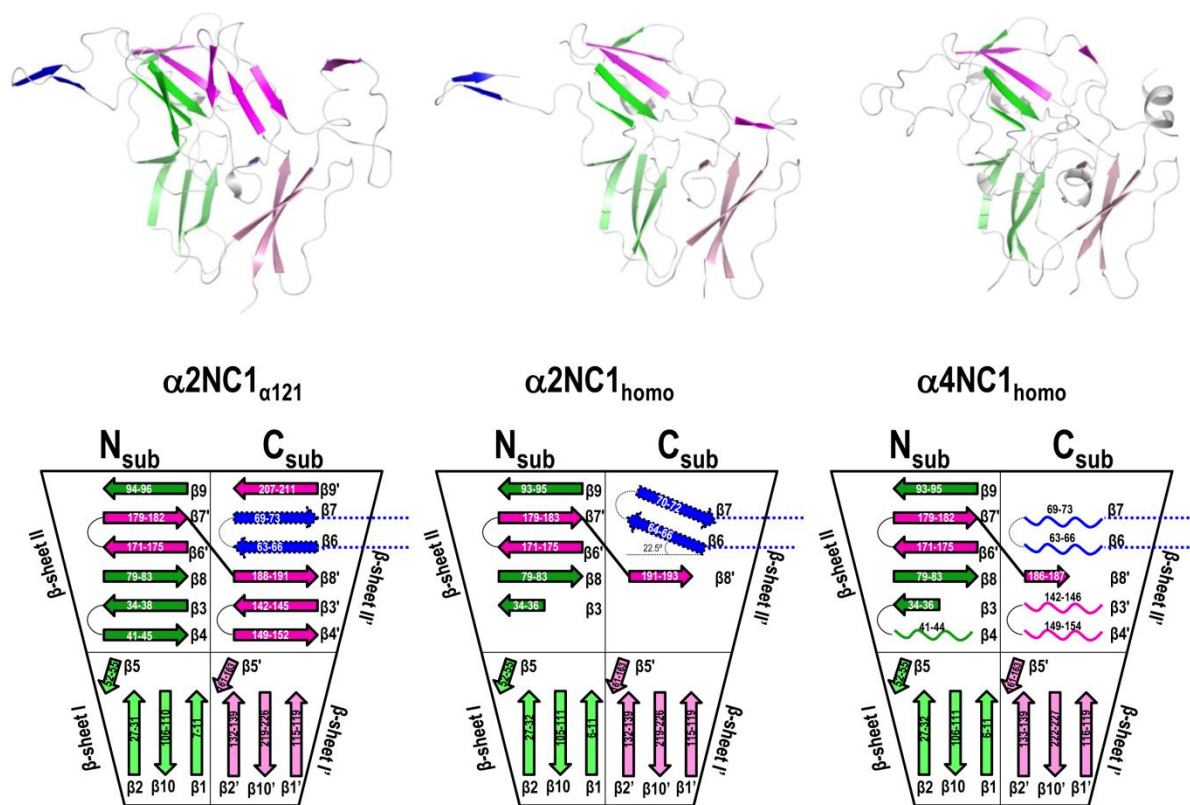


**Figure S6** Cartoon representation of the  $\alpha 2\text{NC1}$  subunit in the  $\alpha 121\text{NC1}$  hexamer ( $\alpha 2\text{NC1}_{\alpha 121}$ ) and the  $\alpha 2\text{NC1}$  and  $\alpha 4\text{NC1}$  domains in the corresponding crystalline homo-oligomers. Below, schemes of the corresponding folds can be seen with the same colour code as in the cartoon representations and labelling of  $\beta$  strands as in Fig 1.

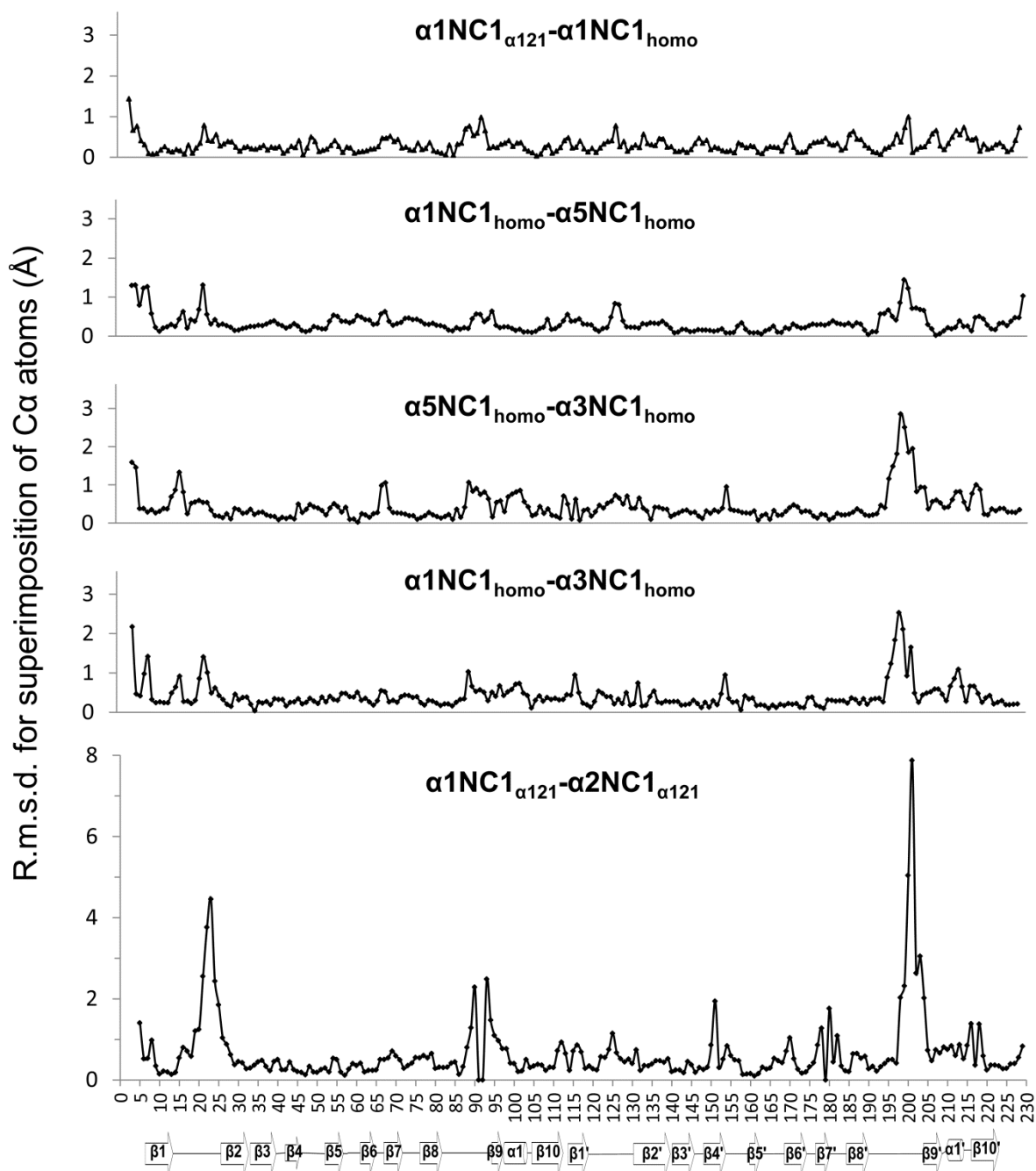


**Figure S7** RMSD value for each Ca atom after superposition of the  $\alpha$ NC1 chains. The residue number and secondary structure of the chains are shown in the X-axis at the bottom.

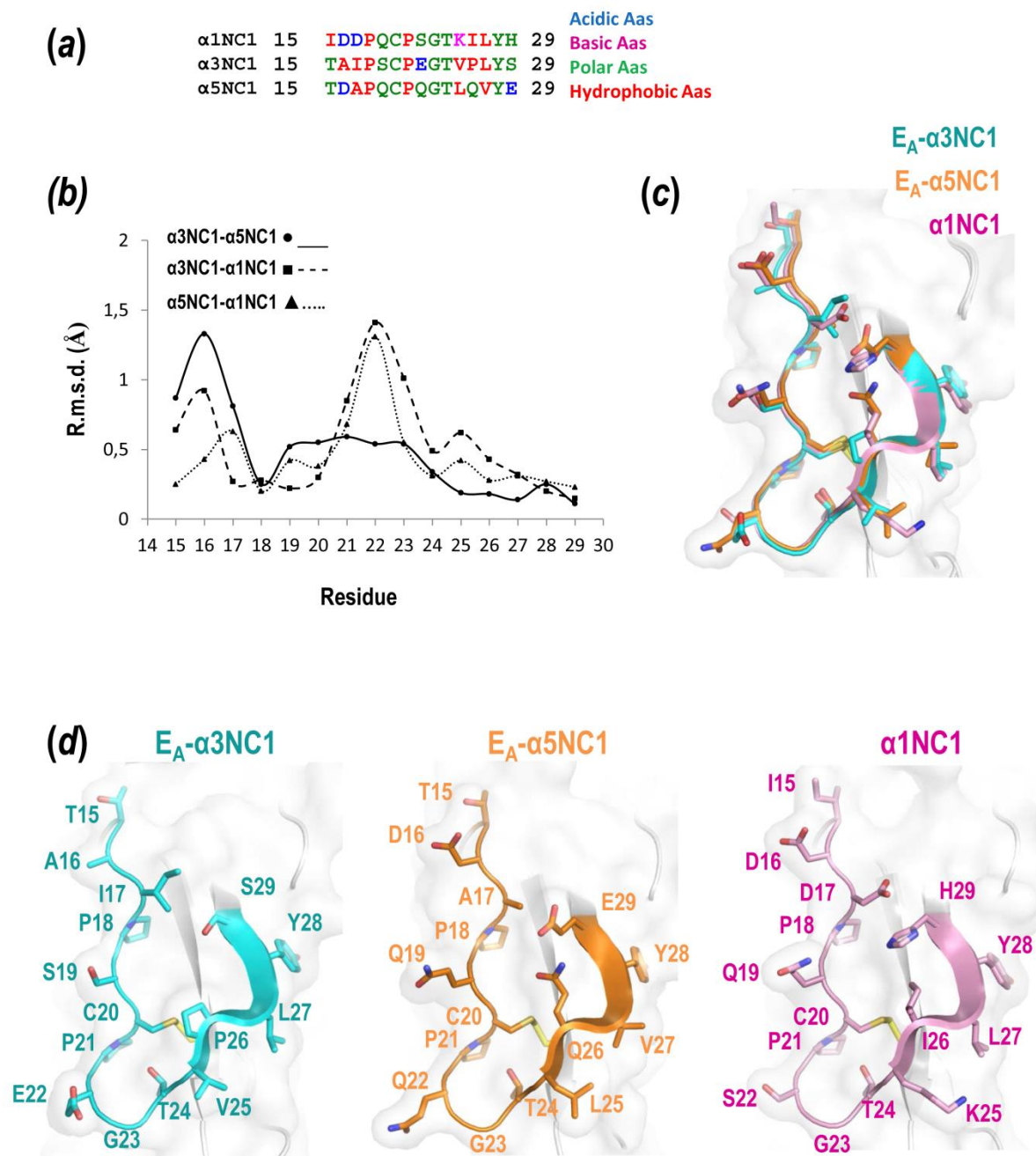


**Figure S8** The Goodpasture's  $E_A$  epitope. (a) Sequence alignment of  $\alpha 3\text{NC1}$  and  $\alpha 5\text{NC1}$  (residues 15-29 of the present structures)  $E_A$  epitopes with the corresponding residues of  $\alpha 1\text{NC1}$  (b) the RMSD values for the superimpositions of the structures corresponding to the sequences aligned in (a) (all from NC1 domains in homo-hexamers). (c) and (d) Cartoon representation of the structural superposition and their individual structures, respectively.

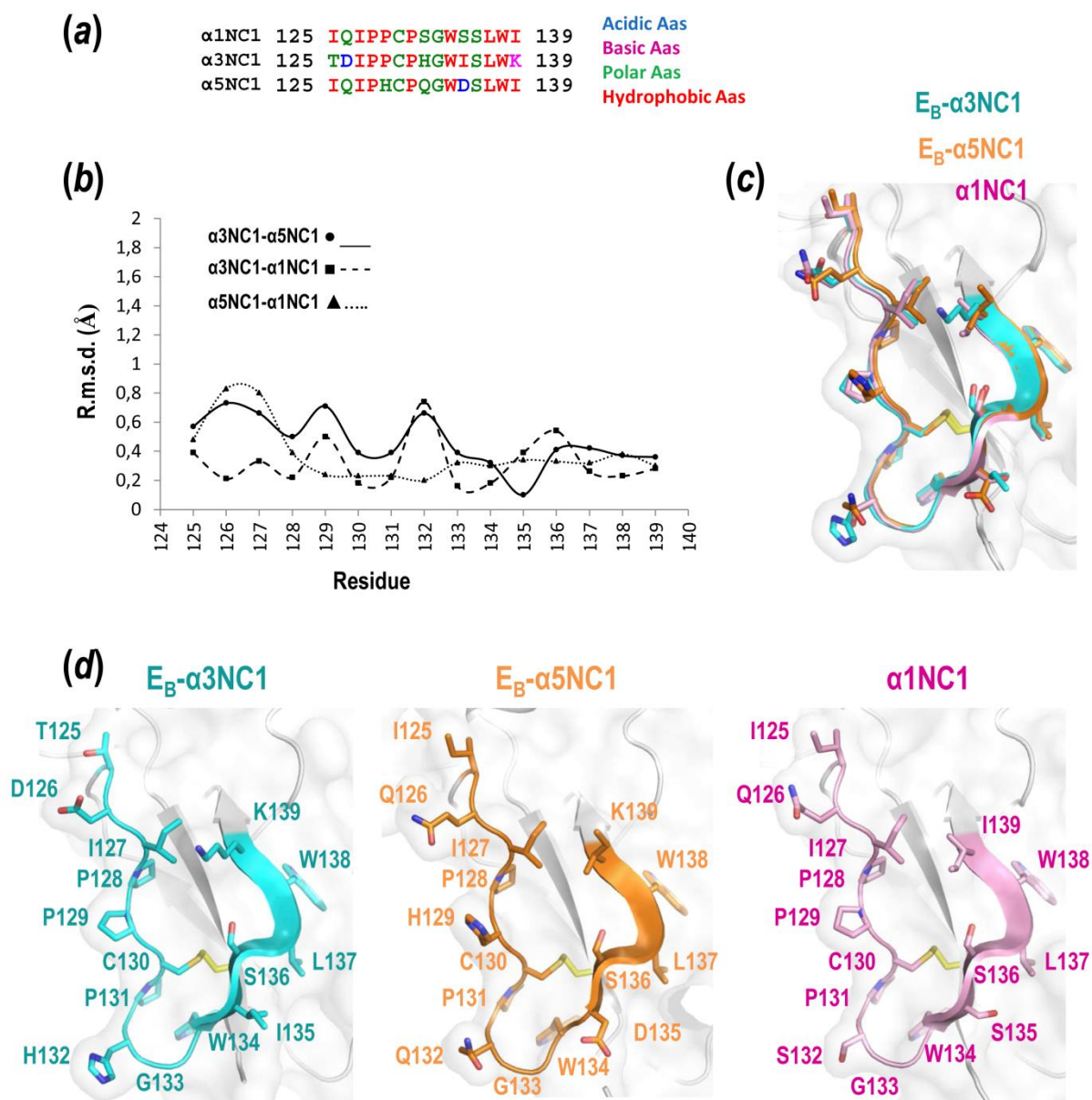


**Figure S9** The Goodpasture's  $E_B$  epitope. (a) Sequence alignment of  $\alpha$ 3NC1 and  $\alpha$ 5NC1 (residues 125-139 of the present structures)  $E_B$  epitopes, with the corresponding residues of  $\alpha$ 1NC1 the RMSD values for the superimpositions of the structures corresponding to the sequences aligned in a (all from NC1 domains in homohexamers). (c) and (d) Cartoon representation of the structural superposition and their individual structures, respectively.

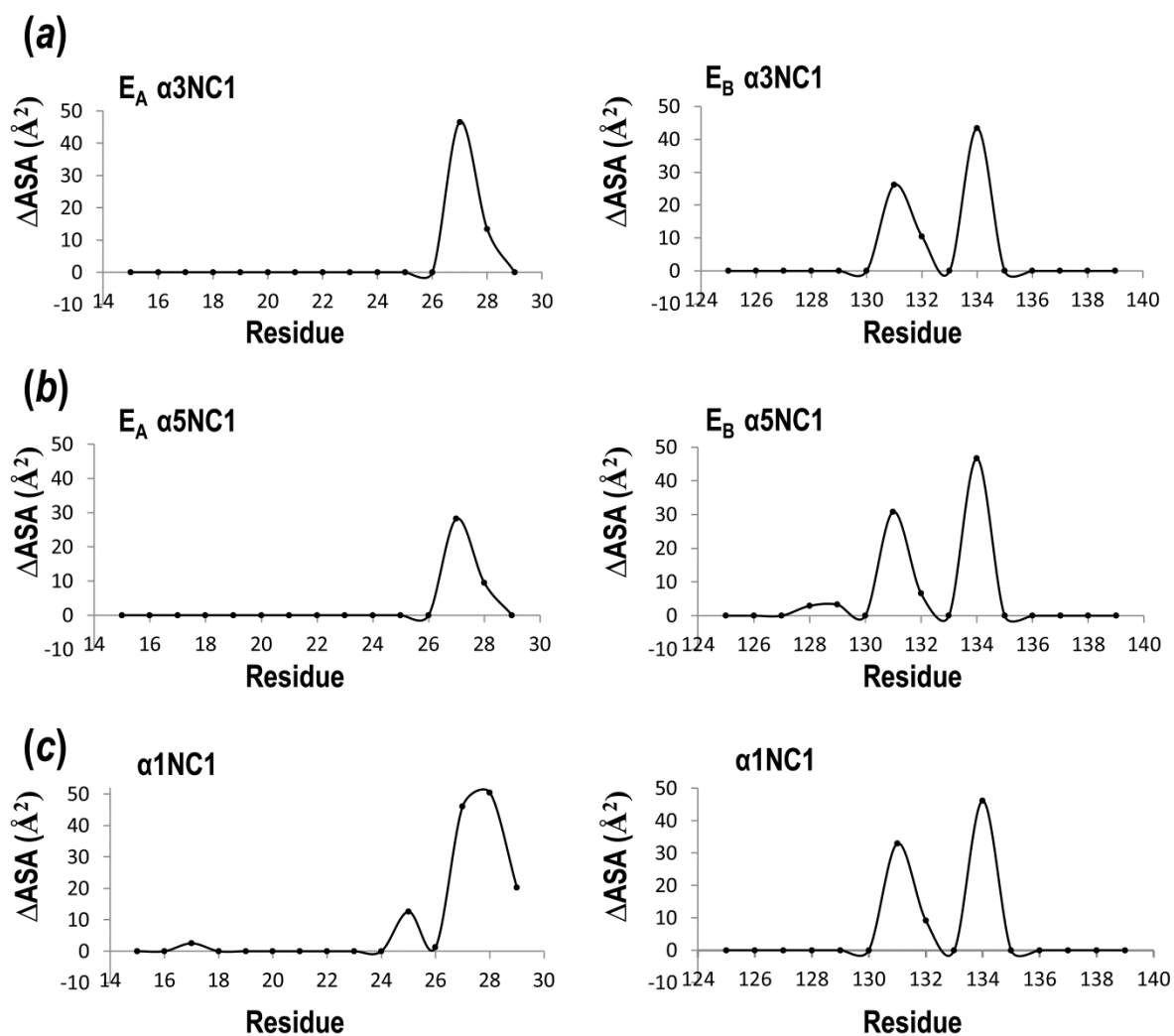


**Figure S10** Accessible surface area difference between monomer and homohexamer ( $\Delta$ ASA) for the E<sub>A</sub> (left) and E<sub>B</sub> (right) epitopes of (a)  $\alpha$ 3NC1 and (b)  $\alpha$ 5NC1 and, for comparison, the corresponding region (c) of  $\alpha$ 1NC1.

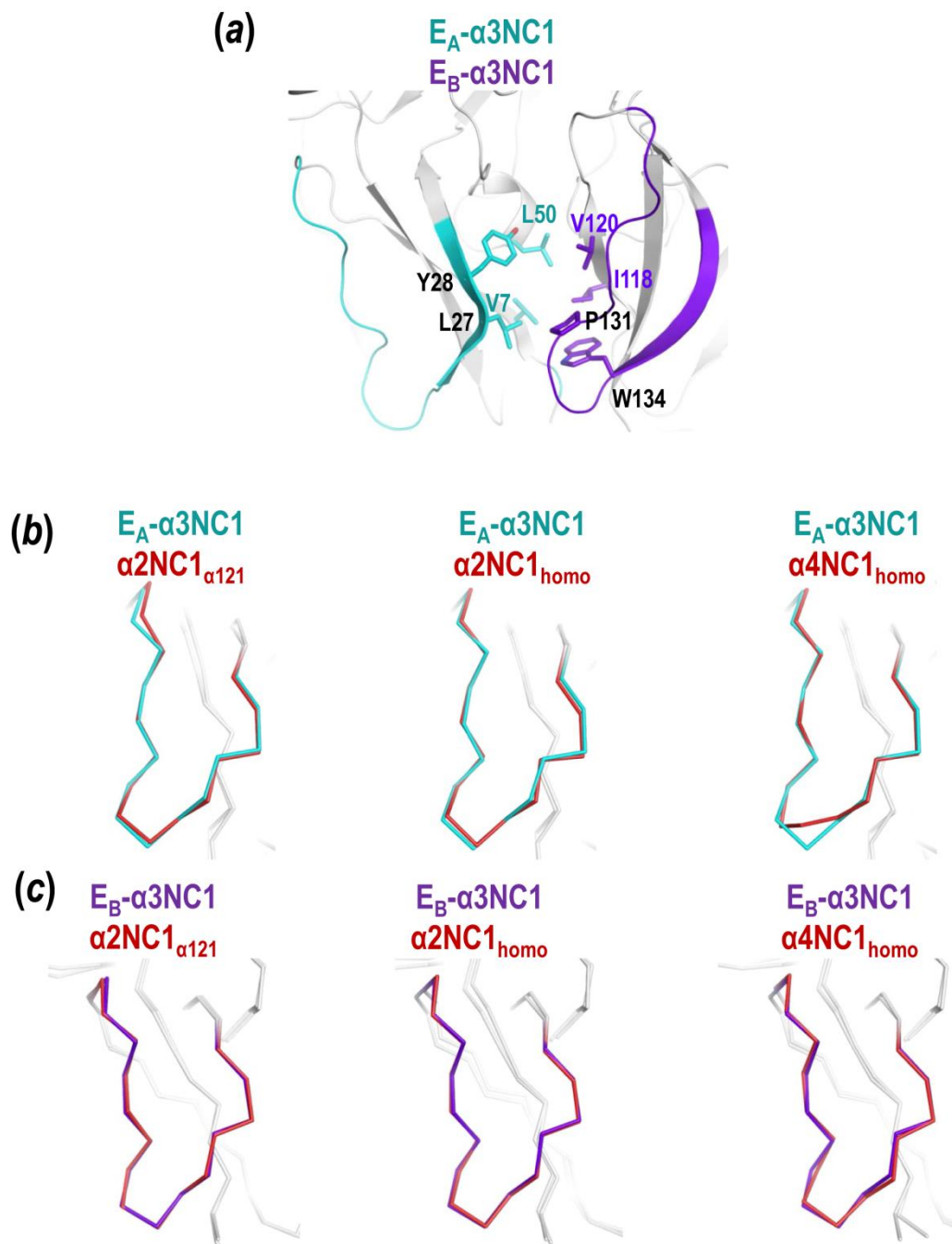


**Figure S11** Hydrophobic patch gluing of  $E_A$  and  $E_B$  epitopes in the  $\alpha 3NC1$  domain structure (a), and illustration of high structural similarity of the two epitopes of  $\alpha 3NC1$  with the corresponding non-autoimmunogenic regions of  $\alpha 2NC1_{\alpha 121}$ ,  $\alpha 2NC1_{\text{homo}}$  and  $\alpha 4NC1_{\text{homo}}$  (b, c).